Chapter 11

MRI vertebral corner inflammation followed by fat deposition is the strongest contributor to the development of new bone at the same vertebral corner: a multi-level longitudinal analysis in patients with ankylosing spondylitis

Machado PM, Baraliakos X, van der Heijde D, Braun J, Landewé R

ANN RHEUM DIS. 2016 AUG;75(8):1486-1493

ABSTRACT

Objectives

To study the sequential relationship between MRI vertebral corner inflammation (VCI), vertebral corner fat deposition (VCFD) and the development/growth of radiographic syndesmophytes at the same vertebral corner (VC).

Methods

Baseline, 24 and 102 weeks spinal MRIs were assessed for the presence/absence of VCI and VCFD. Anterior VCs of lateral radiographs of the cervical and lumbar spine (baseline and 102 weeks) were assessed for the development of new bone (syndesmophyte formation or syndesmophyte formation/growth combined). Data from 161 to 177 patients were analysed at the VC level using two-way and multilevel analyses adjusting for within-patient correlation and MRI reader (generalised estimating equations for binomial outcomes).

Results

The presence of VCI (adjusted (adj) OR 1.75 to 1.98) as well as the presence of VCFD (adjOR 1.60 to 2.32) at any time point (TP) were significantly associated with the development of new bone. The combination of VCI and VCFD at the same VC increased the strength of the association, both for the sequential or simultaneous presence of VCI and VCFD across the three TPs (adjOR 2.12 to 2.73), as well as for the development of new VCFD preceded by VCI at a previous TP (adjOR 2.12 to 3.01). The complete absence of both VCI and VCFD across the three TPs 'protected' against new bone formation (adjOR 0.45 to 0.62). However, 40–66% of new bone still developed in VCs without MRI inflammation or fat degeneration at any of the three TPs.

Conclusion

Both VCI and VCFD contribute to new bone formation in ankylosing spondylitis (AS), especially if VCI precedes VCFD. However, VCI, VCFD and this particular sequence of events only partially explain the development of new bone in AS.

INTRODUCTION

Structural damage in ankylosing spondylitis (AS) is characterised by the formation of new bone in the spine. Syndesmophytes and bridging syndesmophytes are the typical lesions,[1,2] with erosions, sclerosis and squaring being additional lesions that also reflect structural damage in AS. Syndesmophytes can lead to decreased spinal mobility, reduced physical function and loss of quality of life.[3–5] Therefore, understanding the mechanisms underlying new bone formation is of importance in AS.

The processes that drive the formation of new bone in AS are not completely understood, and there is debate about whether inflammation and osteoproliferation are related or uncoupled phenomena.[6–8] This is a challenging topic to investigate because the progression of structural damage is typically slow, it is problematic to perform serial histopathological examinations of spinal tissue and reliable biomarkers of new bone formation in AS are lacking.

MRI provides an indirect and non-invasive method of investigating elements of the pathophysiology of new bone formation in AS. Fat deposition can be seen on T1-weighted sequences and bone marrow oedema (reflecting inflammation) can be seen on T2-weighted sequences with fat suppression, such as the short tau inversion recovery (STIR) sequence.[9–12] However, conventional radiography is still the gold standard method to assess syndesmophyte formation/bridging[13] because tissues with low proton density such as cortical bone and paravertebral ligaments exhibit low or no signal intensity in all pulse sequences and are difficult to differentiate on MRI scans.[14]

It has been shown by us in the same cohort[15] and by others in independent cohorts[16–18] that vertebral corners (VCs)/units/edges with inflammation are more likely to develop new syndesmophytes than VCs/units/edges without inflammation. It has also been proposed that syndesmophytes are more likely to develop at VCs in which inflammation resolves compared with those where inflammation persists.[17,18] Resolving inflammation has also been associated with fat deposition.[19] In turn, fat deposition, with or without concomitant inflammation, has been associated with the formation of new syndesmophytes.[20–22]

Our aim was to expand our analytical studies about the association between inflammation and bone formation by investigating the relationship between MRI inflammation and fat deposition at a VC and the subsequent development of new bone at the same site. In this analysis, the focus was on a sequence analysis, addressing the hypothesis that vertebral corner inflammation (VCI) 'leads to' fat deposition, which in turn 'leads to' bone formation.

METHODS

Study population

For this study, we have made use of the same 80% random sample of the AS Study for the Evaluation of Recombinant Infliximab Therapy (ASSERT) that we used in our previous analysis.[15] Details of the ASSERT study design and population have been previously reported.[23] In brief, ASSERT was a 24-week double-blind placebo-controlled clinical trial with infliximab that included patients with AS (according to the modified New York criteria), with a Bath AS Disease Activity Index[24] (BASDAI) ≥4 (range 0–10) and a spinal pain score ≥4 (range 0–10), with an open extension until 102 weeks with all patients treated with infliximab.

Imaging assessments

Radiographs were scored by two readers at baseline and 102 weeks according to the modified Stoke AS Spine Score (mSASSS).[25] In this study, we used the mSASSS scores from the original ASSERT trial.[23] Lateral views of the cervical and lumbar spine were assessed and anterior VCs from C2-T1 and from T12-S1 (total 24 VCs) were scored for the presence of an erosion, sclerosis or squaring (score 1), syndesmophyte (score 2) or bridging syndesmophyte (score 3). Change from a score of 0 or 1 to 2 or 3 was defined as syndesmophyte formation. Change from a score of 2 to 3 was defined as syndesmophyte growth. The thoracic spine and posterior corners of the cervical and lumbar spine were not assessed because abnormalities at these sites cannot be reliably detected on radiographs.

MRIs were scored by two readers at baseline, 24 and 102 weeks using a VC approach.[9–11] T1-weighted and STIR sequences were assessed and the same 24 VCs scored with the mSASSS were also scored for the presence/absence of VCI and vertebral corner fat deposition (VCFD). The level of agreement between MRI readers regarding the presence/absence of VCI and VCFD was assessed using the kappa statistic. The two MRI readers were different readers than the two X-ray readers and all readers were unaware of the patients' identity, their treatment, the scores of the other imaging modality and the true time-order of the images (fully unbiased scores). This MRI evaluation was a completely new reading, never used in previous ASSERT publications.[15,21,26] Such detailed MRI description of lesions was neither available in the original infliximab efficacy study[26] nor in our previous publication looking at inflammation only (but not fat deposition) at the vertebral unit level (rather than VC level).[15] This new MRI reading was also different from a previous single-reader publication that included the smaller subset of ASSERT patients that were followed up in an investigator-initiated extension study - the European AS Infliximab Cohort.[21]

Imaging longitudinal case definitions

Five case definitions were used to combine the information about the presence/absence of VCI at the three available time points (TPs): (1) VCI at baseline, irrespective of inflammation status at other TPs; (2) VCI at baseline only; (3) VCI at baseline and another TP; (4) VCI at any TP; and (5) VCI at all three TPs. Similar case definitions were applied to the presence/absence of VCFD at the three available TPs (figure 1A).

Six subsequent case definitions (figure 1B) were used to integrate the information about the presence/absence of both VCI and VCFD at the three available TPs: (1) sequential or simultaneous presence of VCI and VCFD across the three TPs (ie, presence of VCI and VCFD at the same or different TPs), (2) presence of VCI but not VCFD across the three TPs, (3) presence of VCFD but not VCI across the three TPs, (4) absence of

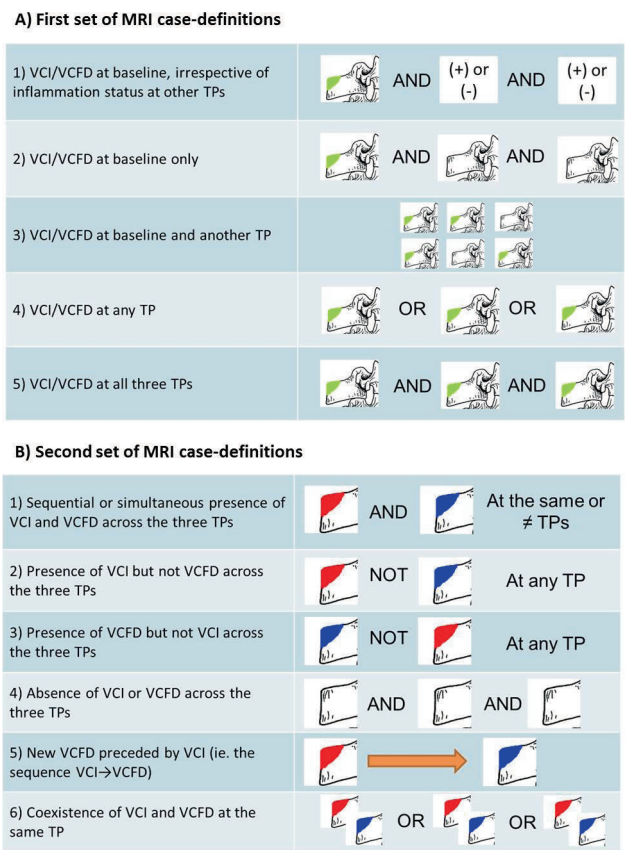

Figure 1. MRI case definitions. (A) MRI case definitions used to combine the information about the presence/absence of vertebral corner inflammation (VCI)/vertebral corner fat deposition (VCFD) at the three available time points (TPs); the green triangle represents VCI or VCFD. (B) MRI case definitions used to integrate the information about the presence/absence of both VCI and VCFD at the three available TPs; the red triangle represents VCI, and the blue triangle represents VCFD.

VCI or VCFD across the three TPs, (5) new VCFD preceded by VCI (ie, the sequence VCI→VCFD) and (6) coexistence of VCI and VCFD at the same TP.

Radiographic data were analysed regarding syndesmophyte formation and regarding syndesmophyte formation/growth combined. Two radiographic case definitions were used in the multilevel approach: (1) one definition aiming at sensitivity: a case was defined as positive if at least one of the readers reported progression of structural damage; and (2) a definition aiming at specificity: a case was defined as positive only if both readers reported progression of structural damage (absolute agreement).

Statistical analysis

Cross-tabulation statistics and measures of association (OR and 95% CI) were first computed using two-way tables to test the association between the various MRI case definitions and radiographic progression after 102 weeks of follow-up. Cross-tabulation statistics were done for every possible pair of imaging readers. The total number of cases in each analysis depended on the imaging case definition and pair of imaging readers used in the analysis (eg, different readers sometimes scored different VCs as not evaluable). Furthermore, VCs with syndesmophytes/ankyloses at baseline (for the outcome syndesmophyte formation) or with ankylosis at baseline (for the outcome syndesmophyte formation/growth) were excluded from the analyses, resulting in another source of variation between readers.

Associations were retested using a multilevel approach to adjust for within-patient correlation and MRI reader (generalised estimating equations (GEEs) for binomial outcomes).[27] The following variables were considered covariates and adjusted for when statistically significant in univariate analysis: gender, age, human leucocyte antigen-B27 status, body mass index, disease duration, presence of syndesmophytes/ankylosis at baseline (at the patient level) and baseline and time-averaged C-reactive protein, BASDAI[24] and AS Disease Activity Score.[28] The treatment variable was forced into all models.

Statistical analyses were performed with IBM SPSS Statistics V.22. Graphics were plotted using GraphPad Prism V.6.

RESULTS

Images belonging to 182 patients with baseline and 102-week radiographic assessments (total of 8736 VCs) and 191 patients with at least one baseline, 24 or 102 weeks MRI assessment (6 patients with one TP, 35 patients with two TPs and 150 patients with three TPs; total of 12624 VCs) were evaluated by the imaging readers. The kappa score

for MRI VCI was 0.46, and the kappa score for MRI VCFD was 0.49. After applying the predefined imaging case definitions and excluding non-evaluable VCs and VCs with syndesmophytes/ankylosis at baseline, data from 3070 to 3389 paired (MRI and radiographic) case definitions belonging to 161–177 patients were analysed. The baseline characteristics of the study population are presented in table 1.

Table 1. Baseline characteristics of the study population (n=177)

Male, no. (%)	141 (79.7)
Age, years	39.0 (32.0, 46.0)
Disease duration, years	9.0 (3.2, 16.1)
BMI, kg/m^2	25.4 (22.6, 27.9)
HLA-B27 positive, no. (%)	160 (90.4)
ASDAS	3.9 (3.3, 4.6)
Time-averaged ASDAS	2.0 (1.4, 2.8)
BASDAI (0–10)	6.5 (5.3, 7.3)
Time-averaged BASDAI (0–10)	3.0 (1.8, 4.9)
CRP, mg/L	15.0 (7.0, 31.0)
Time-averaged CRP, mg/L	3.7 (2.4, 8.1)
mSASSS	13.1 (4.8, 29.5)

Time-averaged values were calculated taking all available time points into account. Except if indicated otherwise, values are the median (IQR). ASDAS, Ankylosing Spondylitis Disease Activity Score; BASDAI, Bath Ankylosing Spondylitis Disease Activity Index; BMI, body mass index; CRP, C-reactive protein; HLA, human leucocyte antigen; mSASSS, modified Stoke Ankylosing Spondylitis Spine Score.

Relationship between VCI and new bone formation

Overall, results showed that the presence of VCI increased the probability of developing new bone at the same VC after 102 weeks of follow-up, irrespective of the MRI case definition, reader pair and radiographic outcome (syndesmophyte formation alone or syndesmophyte formation/growth combined) (supplementary table 1). OR ranged from 1.33 to 3.87 for VCI at baseline, irrespective of inflammation status at other TPs (statistically significant in 7/8 scenarios), 1.46 to 3.86 for VCI at baseline only (statistically significant in 6/8 scenarios), 0.79 to 3.15 for VCI at baseline and another TP (statistically significant in 5/8 scenarios) and 1.19 to 4.10 for VCI at any TP (statistically significant in 7/8 scenarios, figure 2A, B). The analyses for VCI at all TPs were uninterpretable due to the very low number of VCs with persistent inflammation in this tumour necrosis factor (TNF)-blocker treated population.

Relationship between VCFD and new bone formation

Overall, results showed that the presence of VCFD also increased the probability of developing new bone at the same VC after 102 weeks of follow-up. Data were consistent for all reader pairs and for the two definitions of new bone formation (supplementary table 2). The only exception was for the presence of VCFD at baseline only where this trend was not observed. However, the very low number of VCs with VCFD at baseline only,

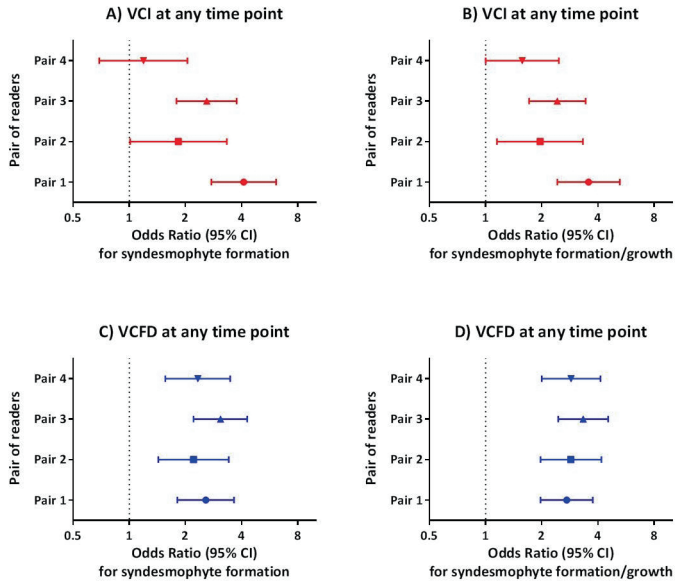

Figure 2. OR (95% CI) of selected vertebral corner inflammation (VCI) or vertebral corner fat deposition (VCFD) MRI case definitions for the outcome syndesmophyte formation (left panel) or syndesmophyte formation/growth (right panel) according to all possible pairs of readers in the two-way analysis. (A) MRI case definition: VCI at any time point, outcome: syndesmophyte formation. (B) MRI case definition: VCI at any time point, outcome: syndesmophyte formation/growth. (C) MRI case definition: VCFD at any time point, outcome: syndesmophyte formation. (D) MRI case definition: VCFD at any time point, outcome: syndesmophyte formation/growth.

makes the interpretation of results difficult. Regarding the other VCFD case definitions, OR ranged from 2.43 to 3.27 for VCFD at baseline, irrespective of fat deposition status at other TPs, 2.62 to 3.37 for VCFD at baseline and another TP, 2.21 to 3.33 for VCFD at any TP (figure 2C, D), and 2.05 to 3.36 for VCFD at all TPs. These associations were statistically significant in all studied scenarios.

Relationship between the various combinations of MRI VCI/VCFD and new bone formation

Supplementary table 3 shows the results for the possible combinations of VCI and VCFD across the three available TPs. The first four MRI case definitions listed in the table are mutually exclusive. The sequential or simultaneous presence of VCI and VCFD across the three TPs was consistently associated with new bone formation (OR 1.77 to 5.80, statistically significant in 7/8 scenarios, figure 3A, B). Associations were weaker for the presence of VCFD but not VCI across the three TPs (OR 1.20 to 2.34, statistically significant in 7/8 scenarios) and even weaker for the presence of VCI but not VCFD across the three TPs (OR 0.40 to 2.32, statistically significant in 2/8 scenarios). The

Table 2. Multivariable GEE results (adjOR; 95% CI) for the outcome syndesmophyte formation or syndesmophyte formation/growth according to X-ray reader 1 or/and reader 2*

Variables	Syndesmophyte formation according to X-ray reader 1 or reader 2					Syndesmophyte formation or growth according to X-ray reader 1 or reader 2				
VCI at any time point	1.98 (1.49, 2.62)	-	-	-	-	1.84 (1.41, 2.41)	-	-	-	-
VCFD at any time point	-	2.32 (1.85, 2.91)	-	-	-	-	2.27 (1.83, 2.81)	-	-	-
Sequential or simultaneous presence of VCI and VCFD across the 3 time points	-	-	2.73 (2.00, 3.74)	-	-	-	-	2.58 (1.91, 3.48)	-	-
New VCFD preceded by VCI	-	-	-	2.45 (1.66, 3.60)	-	-	-	-	2.12 (1.46, 3.08)	-
Absence of VCI or VCFD across the 3 time points	-	-	-	-	0.45 (0.36, 0.56)	-	-	-	-	0.47 (0.38, 0.58)
Treatment (infliximab)	1.03 (0.75, 1.41)	1.09 (0.80, 1.49)	1.02 (0.74, 1.40)	1.05 (0.77, 1.44)	1.04 (0.76, 1.44)	1.15 (0.85, 1.56)	1.23 (0.92, 1.67)	1.18 (0.87, 1.59)	1.14 (0.84, 1.55)	1.18 (0.87, 1.60)
Gender (male)	3.30 (1.94, 5.60)	3.02 (1.79, 5.10)	3.39 (2.01, 5.74)	3.36 (1.98, 5.70)	3.00 (1.77, 5.08)	3.31 (1.96, 5.62)	2.94 (1.75, 4.91)	3.31 (1.96, 5.59)	3.34 (1.98, 5.61)	3.01 (1.79, 5.06)
Syndesmophyte/ankylosis at baseline	2.91 (2.00, 4.25)	2.82 (1.92, 4.13)	2.95 (2.02, 4.29)	2.89 (1.98, 4.21)	2.81 (1.91, 4.11)	3.43 (2.32, 5.08)	3.27 (2.20, 4.85)	3.39 (2.29, 5.01)	3.48 (2.35, 5.14)	3.27 (2.20, 4.85)
Variables	**Syndesmophyte formation according to X-ray reader 1 and reader 2**					**Syndesmophyte formation or growth according to X-ray reader 1 and reader 2**				
VCI at any time point	1.93 (1.22, 3.05)	-	-	-	-	1.75 (1.17, 2.61)	-	-	-	-
VCFD at any time point	-	1.60 (1.10, 2.33)	-	-	-	-	1.85 (1.35, 2.53)	-	-	-
Sequential or simultaneous presence of VCI and VCFD across the 3 time points	-	-	2.29 (1.37, 3.83)	-	-	-	-	2.12 (1.36, 3.31)	-	-
New VCFD preceded by VCI	-	-	-	3.01 (1.76, 5.13)	-	-	-	-	2.17 (1.32, 3.56)	-
Absence of VCI or VCFD across the 3 time points	-	-	-	-	0.62 (0.43, 0.89)	-	-	-	-	0.56 (0.41, 0.76)
Treatment (infliximab)	1.29 (0.68, 2.44)	1.26 (0.66, 2.39)	1.28 (0.67, 2.43)	1.32 (0.70, 2.50)	1.30 (0.68, 2.49)	1.15 (0.63, 2.11)	1.29 (0.72, 2.31)	1.20 (0.66, 2.18)	1.08 (0.59, 2.01)	1.21 (0.66, 2.22)
Gender (male)	2.50 (0.83, 7.51)	2.36 (0.80, 6.97)	2.48 (0.85, 7.26)	2.47 (0.83, 7.33)	2.29 (0.77, 6.77)	3.19 (1.03, 9.91)	2.70 (0.92, 7.88)	3.12 (1.03, 9.50)	3.20 (1.05, 9.74)	2.64 (0.90, 7.80)
Syndesmophyte/ankylosis at baseline	4.11 (1.56, 10.8)	4.22 (1.58, 11.2)	4.19 (1.60, 11.0)	4.14 (1.58, 10.9)	4.18 (1.56, 11.2)	5.45 (2.00, 14.9)	5.65 (2.03, 15.7)	5.50 (2.02, 15.0)	5.54 (2.03, 15.1)	5.53 (1.97, 15.5)

*Results are shown for a selected set of MRI case-definitions and for the adjustment variables: treatment (forced into the model) and gender and presence of syndesmophytes/ankylosis at baseline (the only two other variables significantly associated with new bone formation in univariable analysis); models also adjusted for within-patient correlation by VU-level and MRI-reader. adjOR, adjusted odds ratio; VCI, vertebral corner inflammation; VCFD, vertebral corner fat deposition.

absence of VCI or VCFD across the three TPs was negatively associated with new bone formation (OR 0.33 to 0.49, always statistically significant, figure 3E, F), in agreement with the above positive associations.

The last two MRI case definitions in supplementary table 3 explore two additional settings: new VCFD preceded by VCI (sequence analysis, VCI→VCFD) and the coexistence of

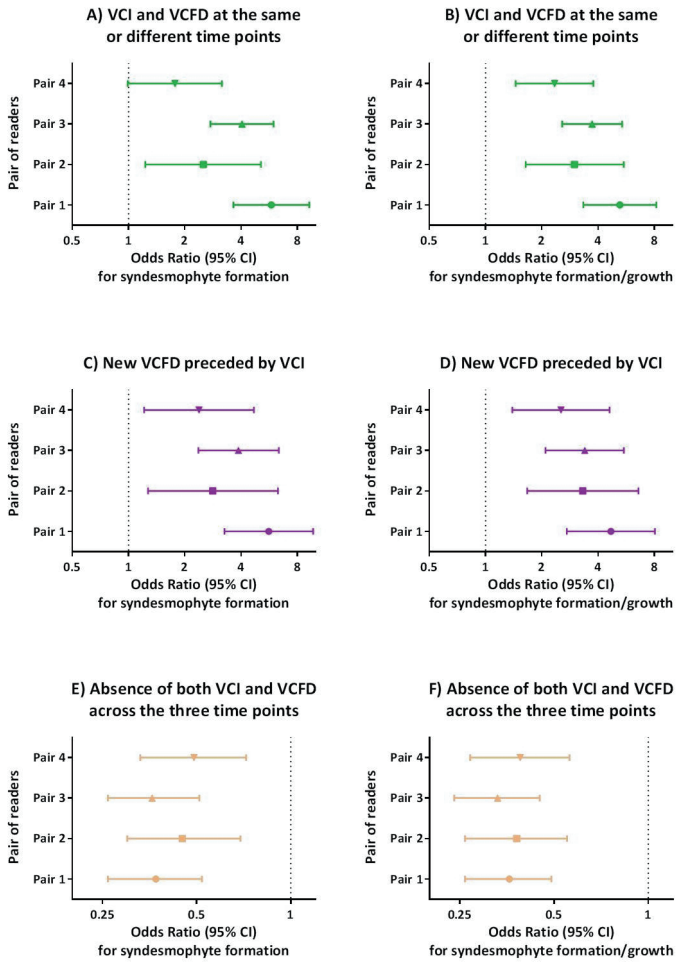

Figure 3. OR (95% CI) of selected combined vertebral corner inflammation (VCI) and vertebral corner fat deposition (VCFD) MRI case definitions for the outcome syndesmophyte formation (left panel) or syndesmophyte formation/growth (right panel) according to all possible pairs of readers in the two-way analysis. (A) MRI case definition: sequential or simultaneous presence of VCI and VCFD across the three time points (ie, presence of VCI and VCFD at the same or different time points), outcome: syndesmophyte formation. (B) MRI case definition: sequential or simultaneous presence of VCI and VCFD across the three time points, outcome: syndesmophyte formation/growth. (C) MRI case definition: new VCFD preceded by VCI, outcome: syndesmophyte formation. (D) MRI case definition: new VCFD

VCFD and VCI at the same TP. VCs in which fat deposition developed de novo and was preceded by VCI showed the highest probability of developing new bone formation (OR 2.38 to 5.62, always statistically significant, figure 3C, D). This relationship was slightly weaker for the coexistence of VCFD and VCI at the same TP (OR 0.85 to 6.00, statistically significant in 5/8 scenarios).

Despite these associations, a large proportion of new bone still developed in VCs without visible MRI inflammation or fat deposition at any of the three assessed TPs (40–66%, depending on the combination of MRI and X-ray reader) (supplementary table 3, percentages can be obtained by using syndesmophyte formation/growth rather than MRI lesions as denominator).

Multilevel GEE analyses

Overall, results of the GEE analyses (supplementary tables 4 and 5) confirmed that both VCI and VCFD are associated with radiographic progression after 102 weeks of follow-up. Results were similar for the outcome syndesmophyte formation and for the outcome syndesmophyte formation/growth combined. The strength and significance of the associations varied depending on the MRI and radiographic case definition. Furthermore, GEE results confirmed that the sequential or simultaneous presence of VCI and VCFD further increases the probability of developing new bone formation, particularly when new VCFD is preceded by VCI (sequence analysis, VCI→VCFD→new bone formation). Some of the most consistent results were observed for VCI at any TP (adjOR 1.75 to 1.98), for VCFD at any TP (adjOR 1.60 to 2.32), for the sequential or simultaneous presence of VCI and VCFD across the three TP (adjOR 2.12 to 2.73) and for new VCFD preceded by VCI (adjOR 2.12 to 3.01). GEE analyses also confirmed that the absence of VCI or VCFD across all TPs 'protects' against new bone formation (adjOR 0.45 to 0.62). These associations were always statistically significant.

The other variables significantly associated with radiographic progression in the GEE multivariable analyses were gender and the presence of syndesmophytes/ankylosis at baseline (at the patient level). Table 2 shows the adjOR for the MRI case definitions most consistently associated with new bone formation as well as the adjOR of the adjustment factors (treatment, gender and the presence of syndesmophytes/ankylosis at baseline). The adjOR for the presence of syndesmophytes/ankylosis at baseline ranged from 2.81 to 5.65, always statistically significant. The adjOR for male gender ranged from 2.36 to 3.39, statistically significant in the majority of cases.

DISCUSSION

In the present study, we have confirmed that MRI VCI is associated with radiographic progression in AS, and we have shown that VCFD is also associated with radiographic progression. In addition, we have shown that the combination of fat and inflammation either at the same TP or sequentially further increases the probability of radiographic progression. Furthermore, VCFD that develops de novo can be preceded by VCI, and this sequence of events is also associated with progression of structural damage. However, VCI, VCFD and this particular sequence only partially explain the development of new bone in AS, as a large proportion of new syndesmophytes/bridging still occurred in VCs without either inflammation or fat deposition across three TPs.

The association between spinal MRI inflammation and radiographic progression after 2 years of follow-up has been reported in four previous studies, including ours.[15–18] OR ranged from 1.7 to 8.6, and differences could be related to methodological aspects such as sample size, type of population (trial/observational cohort, TNF-blocker/standard treatment) and anatomical approach (VC/vertebral unit/vertebral edge). One study has indicated that new syndesmophytes are more likely to develop at VCs where inflammation has completely resolved than at VCs without inflammation at baseline or follow-up.[18] It has also been suggested that VCs with persistent inflammation are less likely to develop new syndesmophytes.[17,18]

The relationship between spinal MRI inflammation, fat deposition and radiographic progression has been assessed in three previous AS studies.[20–22] Chiowchanwisawakit et al[20] showed that VCs that were simultaneously positive for inflammation and fat at baseline had an OR of 7.6 for the development of new syndesmophytes after 2 years of follow-up. Baseline fat and inflammation were both associated with radiographic progression in univariate analysis. However, in multivariable analysis, only the presence of VCI was associated with syndesmophyte formation (OR 5.8). Maksymowych et al[22] studied 'advanced VCI' (defined by the presence of inflammation and concomitant fat, erosion or sclerosis), 'early VCI' (defined by the presence of inflammation only) and VCFD in relation to syndesmophyte formation. When adjusted for the baseline level of damage (at the patient level), only 'advanced VCI' (OR 3.9) and VCFD (OR 4.8) were associated with the development of new syndesmophytes after 2 years of follow-up. However, when both variables were tested in the same model, this association was statistically significant only for VCFD (OR 4.0). Finally, Baraliakos et al[21] found that vertebral edges with both inflammation and fat deposition at baseline had the highest OR (3.7) for syndesmophyte formation after 5 years of follow-up (the reference being vertebral edges without either inflammation or fat at baseline and 2 years). Interestingly, in an axial spondyloarthritis population, Song et al[19] described a significant relationship between the disappearance of inflammation (at the vertebral unit level and using whole-

body MRI) and the development of fat deposition.

It is interesting to discuss our results in relation to the question whether TNF-blockers are capable of inhibiting the progression of structural damage in AS or not. The unexpected lack of inhibition of structural damage by TNF-blockers has fueled the discussion about the relationship between inflammation and new bone formation.[29,30] These initial trial data have recently been challenged by observational studies suggesting a protective effect of TNF-blockers on radiographic progression.[31,32] However, these observational data have important methodological limitations, and this is still an unsolved question.[8] Our observation that the sequence VCI→VCFD is valid and contributes to new bone formation in AS could be supportive of the hypothesis that TNF-blocker treatment in AS may only be effective in protecting from structural damage once newly developed VCI is prevented (after long-term treatment), while the immediate effects of TNF-blocker treatment could paradoxically contribute to new bone formation following the abrupt suppression of VCI and the development of VCFD at the same vertebral corner. However, this equation is more complex because the biological effects of TNF-blockers are not limited to the suppression of inflammation and TNF-blockers have also been associated with osteoproliferation in animal models.[33]

The occurrence of VCFD at baseline only was an infrequent event in our study, and the presence of VCFD at baseline only was not associated with new bone formation. It is possible that in the minority of cases where resolution of VCFD occurs the risk of developing new bone becomes similar to the risk in VCs that never had VCFD. We also observed that VCFD increased at follow-up compared with baseline. Since we analysed a TNF-blocker treated population, this finding would be consistent with the hypothesis that VCFD is more likely to develop at VCs where inflammation resolves compared with VCs with persistent or no inflammation at baseline/follow-up; alternatively, this finding could also simply reflect the natural history of disease, with VCFD being prone to increase over time, irrespective of inflammation.

Consistent with previous studies, we have shown that a significant part of new bone formation occurs in VCs without either traceable inflammation or fat deposition. However, this does not necessarily mean that these VCs do not have inflammation/fat deposition at the microscopic level because MRI may not be sensitive enough to capture all areas of inflammation/fat deposition[34] and because the time between MRI assessments may not be short enough to capture the potential fluctuation of these lesions, particularly inflammation. Conversely, these results could suggest that the mechanisms of new bone formation in AS are still largely unknown and that the triggering of osteoproliferation may be completely or partially independent of inflammation (and fat deposition).[7]

Our study has limitations. First, we analysed a clinical trial cohort of patients with long-standing disease treated with TNF-blockers. Therefore, results cannot be generalised

to patients in earlier disease stages or treated with first line treatments only. Second, two factors that have been shown to influence radiographic progression in AS — non-steroidal anti-inflammatory drug consumption[35 37] and smoking status[38] — could not be adjusted for in our analyses because this information was not available in sufficient detail in the database. Finally, although we have performed MRI assessments at three TPs, additional assessments at shorter intervals may be needed to completely elucidate the dynamics of inflammation and fat deposition over time.

Strengths of our study are the uniquely large population of patients with AS, the large number of imaging readers, the fully unbiased nature of the imaging scoring, the fact that three MRI TPs were analysed (as opposed to one or two TPs as in the majority of previous studies), the fact that we have adjusted for multiple potential confounders using a statistical approach that adjusts for the dependence of observations in the same patient and the comprehensive list of scenarios (case definitions) that have been tested. These strengths make our study the most robust and comprehensive study investigating the relationship between VCI, VCFD and new bone formation to date.

In summary, we have shown that fat deposition in VCs (with or without concomitant inflammation) is associated with radiographic progression and that this association is stronger than for the presence of inflammation alone. Furthermore, inflammatory lesions can precede fat lesions, suggesting the possibility of a window of opportunity to prevent new bone formation. While the longitudinal absence of inflammation and fat deposition was negatively associated with radiographic progression, a significant proportion of new bone still developed at these sites. If this is indeed true and not a consequence of missing inflammation as described above, this suggests that inflammation/fat deposition and new bone formation may reflect independent pathways of the same disease, implying that new therapies specifically targeting osteoproliferation may need to be developed in order to prevent radiographic progression. Interesting future questions are how to incorporate MRI in future clinical trials and long-term observational studies, whether MRI criteria should be incorporated in future treat-to-target treatment strategies and whether new drugs with different mechanisms of action, such as drugs targeting the interleukin (IL)-23/IL-17 axis, will have a different effect in inflammation, fat deposition and structural damage.

REFERENCES

1. Baraliakos X, Listing J, Rudwaleit M, et al. Progression of radiographic damage in patients with ankylosing spondylitis: defining the central role of syndesmophytes. Ann Rheum Dis 2007;66:910–15.
2. Ramiro S, Stolwijk C, van Tubergen A, et al. Evolution of radiographic damage in ankylosing spondylitis: a 12 year prospective follow-up of the OASIS study. Ann Rheum Dis 2015;74:52–9.
3. Machado P, Landewé R, Braun J, et al. Both structural damage and inflammation of the spine contribute to impairment of spinal mobility in patients with ankylosing spondylitis. Ann Rheum Dis 2010;69:1465–70.
4. Machado P, Landewé R, Braun J, et al. A stratified model for health outcomes in ankylosing spondylitis. Ann Rheum Dis 2011;70:1758–64.
5. Landewé R, Dougados M, Mielants H, et al. Physical function in ankylosing spondylitis is independently determined by both disease activity and radiographic damage of the spine. Ann Rheum Dis 2009;68:863–7.
6. Sieper J, Appel H, Braun J, et al. Critical appraisal of assessment of structural damage in ankylosing spondylitis: implications for treatment outcomes. Arthritis Rheum 2008;58:649–56.
7. Lories RJ, Luyten FP, de Vlam K. Progress in spondylarthritis. Mechanisms of new bone formation in spondyloarthritis. Arthritis Res Ther 2009;11:221.
8. Machado P. Anti-tumor necrosis factor and new bone formation in ankylosing spondylitis: the controversy continues. Arthritis Rheum 2013;65:2537–40.
9. Hermann KG, Baraliakos X, van der Heijde DM, et al. Descriptions of spinal MRI lesions and definition of a positive MRI of the spine in axial spondyloarthritis: a consensual approach by the ASAS/OMERACT MRI study group. Ann Rheum Dis 2012;71:1278–88.
10. Lambert RGW, Pedersen SJ, Maksymowych WP, et al. Active inflammatory lesions detected by magnetic resonance imaging in the spine of patients with spondyloarthritis—definitions, assessment system, and reference image set. J Rheumatol 2009;84:3–17.
11. Østergaard M, Maksymowych WP, Pedersen SJ, et al. Structural lesions detected by magnetic resonance imaging in the spine of patients with spondyloarthritis—definitions, assessment system, and reference image set. J Rheumatol 2009;84:18–34.
12. stergaard M, Sørensen IJ. Magnetic resonance imaging—key to understanding and monitoring disease progression in spondyloarthritis? J Rheumatol 2015;42:1–4.
13. Mandl P, Navarro-Compán V, Terslev L, et al. EULAR recommendations for the use of imaging in the diagnosis and management of spondyloarthritis in clinical practice. Ann Rheum Dis 2015;74:1327–39.
14. Han JS, Kaufman B, El Yousef SJ, et al. NMR imaging of the spine. AJR Am J Roentgenol 1983;141:1137–45.
15. van der Heijde D, Machado P, Braun J, et al. MRI inflammation at the vertebral unit only marginally predicts new syndesmophyte formation: a multilevel analysis in patients with ankylosing spondylitis. Ann Rheum Dis 2012;71:369–73.
16. Baraliakos X, Listing J, Rudwaleit M, et al. The relationship between inflammation and new bone formation in patients with ankylosing spondylitis. Arthritis Res Ther 2008;10:R104.
17. Maksymowych WP, Chiowchanwisawakit P, Clare T, et al. Inflammatory lesions of the spine on magnetic resonance imaging predict the development of new syndesmophytes in ankylosing spondylitis: evidence of a relationship between inflammation and new bone formation. Arthritis Rheum 2009;60:93–102.
18. Pedersen SJ, Chiowchanwisawakit P, Lambert RG, et al. Resolution of inflammation following treatment of ankylosing spondylitis is associated with new bone formation. J Rheumatol 2011;38:1349–54.
19. Song IH, Hermann KG, Haibel H, et al. Relationship between active inflammatory lesions in the spine and sacroiliac joints and new development of chronic lesions on whole-body MRI in early axial spondyloarthritis: results of the ESTHER trial at week 48. Ann Rheum Dis 2011;70:1257–63.
20. Chiowchanwisawakit P, Lambert RG, Conner-Spady B, et al. Focal fat lesions at vertebral corners on magnetic resonance imaging predict the development of new syndesmophytes in ankylosing spondylitis. Arthritis Rheum 2011;63:2215–25.
21. Baraliakos X, Heldmann F, Callhoff J, et al. Which spinal lesions are associated with new bone formation in patients with ankylosing spondylitis treated with anti-TNF agents? A long-term observational study using MRI and conventional radiography. Ann Rheum Dis 2014;73:1819–25.
22. Maksymowych WP, Morency N, Conner-Spady B, et al. Suppression of inflammation and effects on new bone formation in ankylosing spondylitis: evidence for a window of opportunity in disease modification. Ann Rheum Dis 2013;72:23–8.
23. van der Heijde D, Dijkmans B, Geusens P, et al. Efficacy and safety of infliximab in patients with ankylosing spondylitis: results of a randomized, placebo-controlled trial (ASSERT). Arthritis

Rheum 2005;52:582–91.

24. Garrett S, Jenkinson T, Kennedy LG, et al. A new approach to defining disease status in ankylosing spondylitis: the Bath Ankylosing Spondylitis Disease Activity Index. J Rheumatol 1994;21:2286–91.
25. Creemers MC, Franssen MJ, van't Hof MA, et al. Assessment of outcome in ankylosing spondylitis: an extended radiographic scoring system. Ann Rheum Dis 2005;64:127–9.
26. Braun J, Landewé R, Hermann KG, et al. Major reduction in spinal inflammation in patients with ankylosing spondylitis after treatment with infliximab: results of a multicenter, randomized, double-blind, placebo-controlled magnetic resonance imaging study. Arthritis Rheum 2006;54:1646–52.
27. Twisk JW. Longitudinal data analysis. A comparison between generalized estimating equations and random coefficient analysis. Eur J Epidemiol 2004;19:769–76. 28.
Machado P, Landewé R, Lie E, et al. Ankylosing Spondylitis Disease Activity Score (ASDAS): defining cut-off values for disease activity states and improvement scores. Ann Rheum Dis 2011;70:47–53.
29. van der Heijde D, Landewé R, Baraliakos X, et al. Radiographic findings following two years of infliximab therapy in patients with ankylosing spondylitis. Arthritis Rheum 2008;58:3063–70.
30. van der Heijde D, Salonen D, Weissman BN, et al. Assessment of radiographic progression in the spines of patients with ankylosing spondylitis treated with adalimumab for up to 2 years. Arthritis Res Ther 2009;11:R127.
31. Haroon N, Inman RD, Learch TJ, et al. The impact of tumor necrosis factor α inhibitors on radiographic progression in ankylosing spondylitis. Arthritis Rheum 2013;65:2645–54.
32. Baraliakos X, Haibel H, Listing J, et al. Continuous long-term anti-TNF therapy does not lead to an increase in the rate of new bone formation over 8 years in patients with ankylosing spondylitis. Ann Rheum Dis 2014;73:710–5.
33. Zwerina J, Tuerk B, Redlich K, et al. Imbalance of local bone metabolism in inflammatory arthritis and its reversal upon tumor necrosis factor blockade: direct analysis of bone turnover in murine arthritis. Arthritis Res Ther 2006;8:R22.
34. Gong Y, Zheng N, Chen SB, et al. Ten years' experience with needle biopsy in the early diagnosis of sacroiliitis. Arthritis Rheum 2012;64:1399–406.
35. Wanders A, Heijde D, Landewé R, et al. Nonsteroidal antiinflammatory drugs reduce radiographic progression in patients with ankylosing spondylitis: a randomized clinical trial. Arthritis Rheum 2005;52:1756–65.
36. Poddubnyy D, Rudwaleit M, Haibel H, et al. Effect of non-steroidal anti-inflammatory drugs on radiographic spinal progression in patients with axial spondyloarthritis: results from the German Spondyloarthritis Inception Cohort. Ann Rheum Dis 2012; 71:1616–22.
37. Kroon F, Landewé R, Dougados M, et al. Continuous NSAID use reverts the effects of inflammation on radiographic progression in patients with ankylosing spondylitis. Ann Rheum Dis 2012;71:1623–9.
38. Poddubnyy D, Haibel H, Listing J, et al. Baseline radiographic damage, elevated acute-phase reactant levels, and cigarette smoking status predict spinal radiographic progression in early axial spondylarthritis. Arthritis Rheum 2012;64:1388–98.

Supplementary table 1. Two-way analysis to test the association between MRI vertebral corner inflammation and new bone formation after 2 years of follow-up*

	New syndesmophyte (X-ray reader 1)		**New syndesmophyte (X-ray reader 2)**		**New syndesmophyte or growth of existing syndesmophyte (X-ray reader 1)**		**New syndesmophyte or growth of existing syndesmophyte (X-ray reader 2)**	
	Yes, No (%)	No, No (%)	Yes, No (%)	No, No (%)	Yes, No (%)	No, No (%)	Yes, No (%)	No, No (%)
Case-definition 1: Vertebral corner inflammation at baseline, irrespective of inflammation status at other time points (MRI reader 1)								
Yes	30 (13.6)	191 (86.4)	12 (5.6)	202 (94.4)	32 (14.3)	191 (85.7)	16 (7.3)	202 (92.7)
No	122 (3.9)	3005 (96.1)	91 (2.9)	3029 (97.1)	146 (4.6)	3005 (95.4)	112 (3.6)	3029 (96.4)
OR (95% CI)	3.87 (2.53, 5.92)		1.98 (1.07, 3.67)		3.49 (2.29, 5.19)		2.14 (1.25, 3.69)	
Case-definition 1: Vertebral corner inflammation at baseline, irrespective of inflammation status at other time points (MRI reader 2)								
Yes	38 (9.8)	350 (90.2)	15 (3.9)	368 (96.1)	43 (10.9)	350 (89.1)	24 (6.1)	368 (93.9)
No	114 (3.9)	2846 (96.1)	88 (3.0)	2863 (97.0)	135 (4.5)	2846 (95.5)	104 (3.5)	2863 (96.5)
OR (95% CI)	**2.71 (1.85, 3.98)**		1.33 (0.76, 2.32)		**2.59 (1.81, 3.72)**		**1.80 (1.14, 2.84)**	
Case-definition 2: Vertebral corner inflammation at baseline only (MRI reader 1)								
Yes	24 (14.5)	141 (85.5)	10 (6.3)	148 (93.7)	26 (15.6)	141 (84.4)	12 (7.5)	148 (92.5)
No	123 (4.2)	2791 (95.8)	89 (3.1)	2823 (96.9)	147 (5.0)	2791 (95.0)	110 (3.8)	2823 (96.2)
OR (95% CI)	3.86 (2.42, 6.17)		2.14 (1.09, 4.21)		3.50 (2.23, 5.49)		2.08 (1.12, 3.86)	
Case-definition 2: Vertebral corner inflammation at baseline only (MRI reader 2)								
Yes	29 (9.7)	270 (90.3)	13 (4.5)	278 (95.5)	33 (10.9)	270 (89.1)	16 (5.4)	278 (94.6)
No	118 (4.2)	2662 (95.8)	86 (3.1)	2693 (96.9)	140 (5.0)	2662 (95.0)	106 (3.8)	2693 (96.2)
OR (95% CI)	**2.42 (1.58, 3.71)**		1.46 (0.81, 2.66)		**2.32 (1.56, 3.47)**		1.46 (0.85, 2.51)	
Case-definition 3: Vertebral corner inflammation at baseline and another time point (MRI reader 1)								
Yes	6 (12.8)	41 (87.2)	2 (4.3)	45 (95.7)	6 (12.8)	41 (87.2)	4 (8.2)	45 (91.8)
No	146 (4.4)	3146 (95.6)	101 (3.1)	3177 (96.9)	172 (5.2)	3146 (94.8)	124 (3.8)	3177 (96.2)
OR (95% CI)	**3.15 (1.32, 7.55)**		1.40 (0.34, 5.84)		**2.68 (1.12, 6.39)**		2.28 (0.81, 6.43)	
Case-definition 3: Vertebral corner inflammation at baseline and another time point (MRI reader 2)								
Yes	9 (11.5)	69 (88.5)	2 (2.5)	79 (97.5)	10 (12.7)	69 (87.3)	8 (9.2)	79 (90.8)
No	143 (4.4)	3116 (95.6)	101 (3.1)	3141 (96.9)	168 (5.1)	3116 (94.9)	120 (3.7)	3141 (96.3)
OR (95% CI)	**2.84 (1.39, 5.81)**		0.79 (0.19, 3.25)		**2.69 (1.36, 5.31)**		**2.65 (1.25, 5.61)**	

	New syndesmophyte (X-ray reader 1)		New syndesmophyte (X-ray reader 2)		New syndesmophyte or growth of existing syndesmophyte (X-ray reader 1)		New syndesmophyte or growth of existing syndesmophyte (X-ray reader 2)	
	Yes, No (%)	No, No (%)	Yes, No (%)	No, No (%)	Yes, No (%)	No, No (%)	Yes, No (%)	No, No (%)
Case-definition 4: Vertebral corner inflammation at any time point (MRI reader 1)								
Yes	36 (14.3)	215 (85.7)	13 (5.4)	229 (94.6)	38 (15.0)	215 (85)	17 (6.9)	229 (93.1)
No	112 (3.9)	2742 (96.1)	86 (3.0)	2768 (97.0)	136 (4.7)	2742 (95.3)	105 (3.7)	2768 (96.3)
OR (95% CI)	4.10 (2.75, 6.12)		1.83 (1.01, 3.33)		3.56 (2.42, 5.24)		1.96 (1.15, 3.32)	
Case-definition 4: Vertebral corner inflammation at any time point (MRI reader 2)								
Yes	43 (9.7)	400 (90.3)	16 (3.7)	419 (96.3)	48 (10.7)	400 (89.3)	25 (5.6)	419 (94.4)
No	106 (4.0)	2559 (96.0)	83 (3.1)	2580 (96.9)	127 (4.7)	2559 (95.3)	98 (3.7)	2580 (96.3)
OR (95% CI)	**2.60 (1.79, 3.76)**		1.19 (0.69, 2.05)		**2.42 (1.71, 3.43)**		**1.57 (1.00, 2.47)**	
Case-definition 5: Vertebral corner inflammation at all three time points (MRI reader 1)								
Yes	1 (25.0)	3 (75.0)	0 (0.0)	4 (100.0)	1 (25.0)	3 (75.0)	0 (0.0)	4 (100.0)
No	151 (4.5)	3208 (95.5)	103 (3.1)	3241 (96.9)	177 (5.2)	177 (5.2)	128 (3.8)	3241 (96.2)
OR (95% CI)	7.08 (0.73, 68.48)		NA		6.04 (0.63, 58.37)		NA	
Case-definition 5: Vertebral corner inflammation at all three time points (MRI reader 2)								
Yes	1 (16.7)	5 (83.3)	0 (0.0)	6 (100.0)	1 (16.7)	5 (83.3)	0 (0.0)	6 (100.0)
No	150 (4.5)	3207 (95.5)	103 (3.1)	3240 (96.9)	176 (5.2)	3207 (94.8)	127 (3.8)	3240 (96.2)
OR (95% CI)	4.28 (0.50, 36.83)		NA		3.64 (0.42, 31.36)		NA	

*In the table cells, the percentage uses new bone formation as numerator and the various definitions of MRI vertebral corner inflammation at the 3 combined time points as denominator. Statistically significant OR ($p<0.05$) are highlighted in **bold.** NA, not applicable.

Supplementary table 2. Two-way analysis to test the association between MRI vertebral corner fat deposition and new bone formation after 2 years' follow-up*

	New syndesmophyte (X-ray reader 1)		**New syndesmophyte (X-ray reader 2)**		**New syndesmophyte or growth of existing syndesmophyte (X-ray reader 1)**		**New syndesmophyte or growth of existing syndesmophyte (X-ray reader 2)**	
	Yes, No (%)	No, No (%)	Yes, No (%)	No, No (%)	Yes, No (%)	No, No (%)	Yes, No (%)	No, No (%)
Case-definition 1: Vertebral corner fat deposition at baseline, irrespective of fat deposition status at other time points (MRI reader 1)								
Yes	25 (9.4)	240 (90.6)	19 (7.2)	244 (92.8)	32 (11.8)	240 (88.2)	27 (10.0)	244 (90.0)
No	127 (4.1)	2956 (95.9)	84 (2.7)	2987 (97.3)	146 (4.7)	2956 (95.3)	101 (3.3)	2987 (96.7)
OR (95% CI)	2.43 (1.55, 3.80)		2.77 (1.66, 4.63)		2.70 (1.80, 4.05)		3.27 (2.10, 5.10)	
Case-definition 1: Vertebral corner fat deposition at baseline, irrespective of fat deposition status at other time points (MRI reader 1)								
Yes	54 (9.6)	508 (90.4)	34 (6.1)	524 (93.9)	65 (11.3)	508 (88.7)	45 (7.9)	524 (92.1)
No	98 (3.5)	2688 (96.5)	69 (2.5)	2707 (97.5)	113 (4.0)	2688 (96.0)	83 (3.0)	2707 (97.0)
OR (95% CI)	2.92 (2.06, 4.12)		2.55 (1.67, 3.88)		3.04 (2.21, 4.19)		2.80 (1.93, 4.07)	
Case-definition 2: Vertebral corner fat deposition at baseline only (MRI reader 1)								
Yes	0 (0.0)	11 (100)	1 (8.3)	11 (91.7)	0 (0.0)	11 (100.0)	1 (8.3)	11 (91.7)
No	147 (4.8)	2921 (95.2)	98 (3.2)	2960 (96.8)	173 (5.6)	2921 (94.4)	121 (3.9)	2960 (96.1)
OR (95% CI)	NA		2.75 (0.35, 21.48)		NA		2.22 (0.29, 17.37)	
Case-definition 2: Vertebral corner fat deposition at baseline only (MRI reader 2)								
Yes	4 (10.0)	36 (90.0)	1 (2.4)	40 (97.6)	4 (10.0)	36 (90.0)	1 (2.4)	40 (97.6)
No	143 (4.7)	2896 (95.3)	98 (3.2)	2931 (96.8)	169 (5.5)	2896 (94.5)	121 (4.0)	2931 (96.0)
OR (95% CI)	2.25 (0.79, 6.41)		0.75 (0.10, 5.49)		1.90 (0.67, 5.41)		0.61 (0.08, 4.44)	
Case-definition 3: Vertebral corner fat deposition at baseline and another time point (MRI reader 1)								
Yes	25 (10.1)	223 (89.9)	18 (7.3)	227 (92.7)	32 (12.5)	223 (87.5)	26 (10.3)	227 (89.7)
No	127 (4.1)	2967 (95.9)	85 (2.8)	2998 (97.2)	146 (4.7)	2967 (95.3)	102 (3.3)	2998 (96.7)
OR (95% CI)	2.62 (1.67, 4.11)		2.80 (1.65, 4.73)		2.92 (1.94, 4.38)		3.37 (2.14, 5.29)	
Case-definition 3: Vertebral corner fat deposition at baseline and another time point (MRI reader 2)								
Yes	48 (9.5)	457 (90.5)	33 (6.6)	469 (93.4)	59 (11.4)	457 (88.6)	42 (8.2)	469 (91.8)
No	102 (3.6)	2724 (96.4)	70 (2.5)	2747 (97.5)	117 (4.1)	2724 (95.9)	84 (3.0)	2747 (97.0)
OR (95% CI)	2.81 (1.96, 4.01)		2.76 (1.81, 4.23)		3.01 (2.17, 4.17)		2.93 (2.00, 4.30)	

	New syndesmophyte (X-ray reader 1)		New syndesmophyte (X-ray reader 2)		New syndesmophyte or growth of existing syndesmophyte (X-ray reader 1)		New syndesmophyte or growth of existing syndesmophyte (X-ray reader 2)	
	Yes, No (%)	No, No (%)	Yes, No (%)	No, No (%)	Yes, No (%)	No, No (%)	Yes, No (%)	No, No (%)
Case-definition 4: Vertebral corner fat deposition at any time point (MRI reader 1)								
Yes	51 (9.5)	487 (90.5)	31 (5.8)	508 (94.2)	62 (11.3)	487 (88.7)	46 (8.3)	508 (91.7)
No	101 (3.9)	2475 (96.1)	69 (2.7)	2497 (97.3)	116 (4.5)	2475 (95.5)	79 (3.1)	2497 (96.9)
OR (95% CI)	2.57 (1.81, 3.64)		2.21 (1.43, 3.41)		2.72 (1.97, 3.75)		2.86 (1.97, 4.17)	
Case-definition 4: Vertebral corner fat deposition at any time point (MRI reader 2)								
Yes	85 (8.9)	869 (91.1)	50 (5.2)	907 (94.8)	103 (10.6)	869 (89.4)	69 (7.1)	907 (92.9)
No	67 (3.1)	2109 (96.9)	50 (2.3)	2111 (97.7)	75 (3.4)	2109 (96.6)	56 (2.6)	2111 (97.4)
OR (95% CI)	3.08 (2.21, 4.28)		2.33 (1.56, 3.47)		3.33 (2.45, 4.53)		2.87 (2.00, 4.12)	
Case-definition 5: Vertebral corner fat deposition at all three time points (MRI reader 1)								
Yes	17 (8.2)	190 (91.8)	16 (7.7)	193 (92.3)	23 (10.8)	190 (89.2)	22 (10.2)	193 (89.8)
No	131 (4.2)	3007 (95.8)	86 (2.8)	3035 (97.2)	151 (4.8)	3007 (95.2)	103 (3.3)	3035 (96.7)
OR (95% CI)	2.05 (1.21, 3.48)		2.93 (1.68, 5.09)		2.41 (1.52, 3.83)		3.36 (2.07, 5.44)	
Case-definition 5: Vertebral corner fat deposition at all three time points (MRI reader 2)								
Yes	31 (9.1)	309 (90.9)	24 (6.9)	322 (93.1)	38 (11.0)	309 (89.0)	31 (8.8)	322 (91.2)
No	119 (4.0)	2884 (96.0)	78 (2.6)	2905 (97.4)	138 (4.6)	2884 (95.4)	96 (3.2)	2905 (96.8)
OR (95% CI)	2.43 (1.61, 3.67)		2.78 (1.73, 4.45)		2.57 (1.76, 3.75)		2.91 (1.91, 4.44)	

*In the table cells, the percentage uses new bone formation as numerator and the various definitions of MRI vertebral corner fat deposition at the 3 combined time points as denominator. Statistically significant OR ($p<0.05$) are highlighted in **bold.** NA, not applicable.

Supplementary table 3. Two-way analysis to test the association between the various combinations of MRI vertebral corner inflammation and fat deposition taking the three time points into account and new bone formation after 2 years follow-up*

	New syndesmophyte (X-ray reader 1)		**New syndesmophyte (X-ray reader 2)**		**New syndesmophyte or growth of existing syndesmophyte (X-ray reader 1)**		**New syndesmophyte or growth of existing syndesmophyte (X-ray reader 2)**	
	Yes, No (%)	No, No (%)	Yes, No (%)	No, No (%)	Yes, No (%)	No, No (%)	Yes, No (%)	No, No (%)
Case-definition 1: Sequential or simultaneous presence of vertebral corner inflammation and fat deposition across the 3 time points (MRI reader 1)								
Yes	26 (20.0)	104 (80.0)	9 (7.3)	114 (92.7)	28 (21.2)	104 (78.8)	13 (10.2)	114 (89.8)
No	122 (4.1)	2831 (95.9)	90 (3.0)	2861 (97.0)	146 (4.9)	2831 (95.1)	109 (3.7)	2861 (96.3)
OR (95% CI)	5.80 (3.64, 9.25)		2.51 (1.23, 5.11)		5.22 (3.33, 8.18)		2.99 (1.64, 5.48)	
Case-definition 1: Sequential or simultaneous presence of vertebral corner inflammation and fat deposition across the 3 time points (MRI reader 2)								
Yes	39 (14.1)	237 (85.8)	14 (5.2)	254 (94.8)	43 (15.4)	237 (84.6)	22 (8.0)	254 (92.0)
No	110 (3.9)	2702 (96.1)	85 (3.0)	2725 (97.0)	132 (4.7)	2702 (95.3)	101 (3.6)	2725 (96.4)
OR (95% CI)	**4.04 (2.74, 5.96)**		1.77 (0.99, 3.16)		**3.71 (2.57, 5.37)**		**2.34 (1.45, 3.77)**	
Case-definition 2: Presence of vertebral corner inflammation but not fat deposition across the 3 time points (MRI reader 1)								
Yes	10 (10.1)	89 (89.9)	4 (4.1)	93 (95.9)	10 (10.1)	89 (89.9)	4 (4.1)	93 (95.9)
No	138 (4.6)	2846 (95.4)	95 (3.2)	2882 (96.8)	164 (5.4)	2846 (94.6)	118 (3.9)	2882 (96.1)
OR (95% CI)	2.32 (1.18, 4.55)		1.31 (0.47, 3.62)		**1.95 (1.00, 3.82)**		1.05 (0.38, 2.91)	
Case-definition 2: Presence of vertebral corner inflammation but not fat deposition across the 3 time points (MRI reader 2)								
Yes	4 (2.7)	143 (97.3)	2 (1.4)	145 (98.6)	5 (3.4)	143 (96.6)	3 (2.0)	145 (98.0)
No	145 (4.9)	2796 (95.1)	97 (3.3)	2834 (96.7)	170 (5.7)	2796 (94.3)	120 (4.1)	2834 (95.9)
OR (95% CI)	0.54 (0.20, 1.48)		0.40 (0.10, 1.65)		0.58 (0.23, 1.42)		0.49 (0.15, 1.56)	
Case-definition 3: Presence of vertebral corner fat deposition but not inflammation across the 3 time points (MRI reader 1)								
Yes	21 (5.6)	356 (94.4)	21 (5.5)	364 (94.5)	30 (7.8)	356 (92.2)	30 (7.6)	364 (92.4)
No	127 (4.7)	2579 (95.3)	78 (2.9)	2611 (97.1)	144 (5.3)	2579 (94.4)	92 (3.4)	2611 (96.6)
OR (95% CI)	1.20 (0.75, 1.93)		**1.93 (1.18, 3.17)**		1.51 (1.00, 2.27)		2.34 (1.53, 3.58)	
Case-definition 3: Presence of vertebral corner fat deposition but not inflammation across the 3 time points (MRI reader 2)								
Yes	43 (6.8)	593 (93.2)	35 (5.4)	614 (94.6)	57 (8.8)	593 (91.2)	45 (6.8)	614 (93.2)
No	106 (4.3)	2346 (95.7)	64 (2.6)	2365 (97.4)	118 (4.8)	2346 (95.2)	78 (3.2)	2365 (96.8)
OR (95% CI)	1.61 (1.11, 2.31)		2.11 (1.38, 3.21)		1.91 (1.38, 2.66)		2.22 (1.52, 3.24)	

	New syndesmophyte (X-ray reader 1)		New syndesmophyte (X-ray reader 2)		New syndesmophyte or growth of existing syndesmophyte (X-ray reader 1)		New syndesmophyte or growth of existing syndesmophyte (X-ray reader 2)	
	Yes, No (%)	No, No (%)	Yes, No (%)	No, No (%)	Yes, No (%)	No, No (%)	Yes, No (%)	No, No (%)
Case-definition 4: Absence of vertebral corner inflammation or fat deposition across the 3 time points (MRI reader 1)								
Yes	91 (3.7)	2386 (96.3)	65 (2.6)	2404 (97.4)	106 (4.3)	2386 (95.7)	75 (3.0)	2404 (97.0)
No	57 (9.4)	549 (90.6)	34 (5.6)	571 (94.4)	68 (11.0)	549 (89.0)	47 (7.6)	571 (92.4)
OR (95% CI)	0.37 (0.26, 0.52)		0.45 (0.30, 0.69)		0.36 (0.26, 0.49)		0.38 (0.26, 0.55)	
Case-definition 4: Absence of vertebral corner inflammation or fat deposition across the 3 time points (MRI reader 2)								
Yes	63 (3.1)	1966 (96.9)	48 (2.4)	1966 (97.6)	70 (3.4)	1966 (96.6)	53 (2.6)	1966 (97.4)
No	86 (8.1)	973 (91.9)	51 (4.8)	1013 (95.2)	105 (9.7)	973 (90.3)	70 (6.5)	1013 (93.5)
OR (95% CI)	0.36 (0.26, 0.51)		0.49 (0.33, 0.72)		0.33 (0.24, 0.45)		0.39 (0.27, 0.56)	
Case-definition 5: New vertebral corner fat deposition preceded by vertebral corner inflammation (MRI reader 1)								
Yes	18 (20.2)	71 (79.8)	7 (8.2)	78 (91.8)	18 (20.2)	71 (79.8)	10 (11.4)	78 (88.6)
No	129 (4.3)	2861 (95.7)	92 (3.1)	2893 (96.9)	155 (5.1)	2861 (94.9)	112 (3.7)	2893 (96.3)
OR (95% CI)	5.62 (3.26, 9.71)		2.82 (1.27, 6.29)		4.68 (2.72, 8.05)		3.31 (1.67, 6.57)	
Case-definition 5: New vertebral corner fat deposition preceded by vertebral corner inflammation (MRI reader 2)								
Yes	21 (14.8)	121 (85.2)	10 (6.9)	134 (93.1)	22 (15.4)	121 (84.6)	13 (8.8)	134 (91.2)
No	126 (4.3)	2811 (95.7)	89 (3.0)	2837 (97.0)	151 (5.1)	2811 (94.9)	109 (3.7)	2837 (96.3)
OR (95% CI)	3.87 (2.36, 6.36)		2.38 (1.21, 4.68)		3.39 (2.09, 5.49)		2.53 (1.39, 4.60)	
Case-definition 6: Coexistence of vertebral corner fat deposition and inflammation at the same time point (MRI reader 1)								
Yes	10 (21.7)	36 (78.3)	2 (4.9)	39 (95.1)	12 (25)	36 (75)	3 (7.1)	39 (92.9)
No	137 (4.5)	2899 (95.5)	97 (3.2)	2935 (96.8)	161 (5.3)	2899 (94.7)	119 (3.9)	2935 (96.1)
OR (95% CI)	**5.88 (2.86, 12.09)**		1.55 (0.37, 6.52)		**6.00 (3.06, 11.76)**		1.90 (0.58, 6.23)	
Case-definition 6: Coexistence of vertebral corner fat deposition and inflammation at the same time point (MRI reader 2)								
Yes	20 (13.2)	132 (86.8)	4 (2.8)	140 (97.2)	23 (14.8)	132 (85.2)	10 (6.7)	140 (93.3)
No	128 (4.4)	2806 (95.6)	95 (3.2)	2837 (96.8)	151 (5.1)	2806 (94.9)	113 (3.8)	2837 (96.2)
OR (95% CI)	**3.32 (2.01, 5.49)**		0.85 (0.31, 2.35)		**3.24 (2.02, 5.19)**		**1.79 (0.92, 3.50)**	

*In the table cells, the percentage uses new bone formation as numerator and the various definitions of combined MRI vertebral corner inflammation and fat deposition as denominator. Statistically significant OR ($p<0.05$) are highlighted in **bold.**

Supplementary table 4. GEE results (adjOR; 95% CI; p values) for the outcome syndesmophyte formation (upper section) and for the outcome syndesmophyte formation or growth of existing syndesmophytes (lower section) according to X-ray reader 1 or reader 2

Definitions of VCI or VCFD	Syndesmophyte formation according to X-ray reader 1 or reader 2	
	Adjustment for within-patient correlation by VU-level and MRI-reader	**Multivariable adjustment***
Definitions based on the presence of VCI and taking the 3 TPs into account		
VCI at baseline, irrespective of inflammation status at other TPs	2.23 (1.65, 3.00); p<0.001	1.95 (1.45, 2.62); p<0.001
VCI at baseline only	2.04 (1.48, 2.82); p<0.001	1.90 (1.37, 2.63); p<0.001
VCI at baseline and another TP	1.89 (1.04, 3.42); p=0.036	1.62 (0.91, 2.90); p=0.102
VCI at any TP	2.21 (1.68, 2.93); p<0.001	1.98 (1.49, 2.62); p<0.001
Definitions based on the presence of VCFD and taking the 3 TPs into account		
VCFD at baseline, irrespective of inflammation status at other TPs	2.66 (2.08, 3.41); p<0.001	2.47 (1.93, 3.17); p<0.001
VCFD at baseline only	1.92 (0.85, 4.34); p=0.118	1.76 (0.75, 4.12); p=0.193
VCFD at baseline and another TP	2.65 (2.05, 3.41); p<0.001	2.45 (1.90, 3.17); p<0.001
VCFD at any TP	2.59 (2.07, 3.24); p<0.001	2.32 (1.85, 2.91); p<0.001
VCFD at all TPs	2.49 (1.87, 3.31); p<0.001	2.30 (1.73, 3.06); p<0.001
Combined definitions based on the presence of VCI and VCFD and taking the 3 TPs into account		
Sequential or simultaneous presence of VCI and VCFD across the 3 TPs	3.02 (2.22, 4.12); p<0.001	2.73 (2.00, 3.74); p<0.001
Presence of VCI but not VCFD across the 3 TPs	1.04 (0.62, 1.75); p=0.883	0.97 (0.57, 1.64); p=0.905
Presence of VCFD but not VCI across the 3 TPs	1.76 (1.38, 2.24); p<0.001	1.60 (1.25, 2.04); p<0.001
Absence of VCI or VCFD across the 3 TPs	0.40 (0.32, 0.50); p<0.001	0.45 (0.36, 0.56); p<0.001
New VCFD preceded by VCI	2.59 (1.76, 3.80); p<0.001	2.45 (1.66, 3.60); p<0.001
Coexistence of VCFD and VCI at the same TP	2.64 (1.73, 4.02); p<0.001	2.37 (1.55, 3.63); p<0.001

Definitions of VCI or VCFD	Syndesmophyte formation or growth according to X-ray reader 1 or reader 2	
	Adjustment for within-patient correlation by VU-level and MRI-reader	**Multivariable adjustment***
Definitions based on the presence of VCI and taking the 3 TPs into account		
VCI at baseline, irrespective of inflammation status at other TPs	2.10 (1.58, 2.78); p<0.001	1.88 (1.42, 2.50); p<0.001
VCI at baseline only	1.76 (1.29; 2.40); p<0.001	1.70 (1.24, 2.33); p=0.001
VCI at baseline and another TP	2.10 (1.25; 3.53); p=0.005	1.83 (1.09, 3.04); p=0.021
VCI at any TP	2.01 (1.55, 2.62); p<0.001	1.84 (1.41, 2.41); p<0.001
Definitions based on the presence of VCFD and taking the 3 TPs into account		
VCFD at baseline, irrespective of inflammation status at other TPs	2.59 (2.07, 3.26); p<0.001	2.46 (1.95, 3.10); p<0.001
VCFD at baseline only	1.83 (0.86, 3.88); p=0.118	1.63 (0.73, 3.66); p=0.233
VCFD at baseline and another TP	2.59 (2.05, 3.27); p<0.001	2.45 (1.93, 3.12); p<0.001
VCFD at any TP	2.47 (2.00, 3.04); p<0.001	2.27 (1.83, 2.81); p<0.001
VCFD at all TPs	2.44 (1.88, 3.17); p<0.001	2.31 (1.77, 3.01); p<0.001
Combined definitions based on the presence of VCI and VCFD and taking the 3 TPs into account		
Sequential or simultaneous presence of VCI and VCFD across the 3 TPs	2.77 (2.07, 3.72); p<0.001	2.58 (1.91, 3.48); p<0.001
Presence of VCI but not VCFD across the 3 TPs	0.92 (0.56, 1.51); p=0.732	0.87 (0.52, 1.45); p=0.590
Presence of VCFD but not VCI across the 3 TPs	1.74 (1.40, 2.18); p<0.001	1.63 (1.29, 2.05); p<0.001
Absence of VCI or VCFD across the 3 TPs	0.43 (0.35, 0.53); p<0.001	0.47 (0.38, 0.58); p<0.001
New VCFD preceded by VCI	2.16 (1.49, 3.13); p<0.001	2.12 (1.46, 3.08); p<0.001
Coexistence of VCFD and VCI at the same TP	2.58 (1.75, 3.82); p<0.001	2.40 (1.61, 3.57); p<0.001

*Adjustment for within-patient correlation by VU-level and MRI-reader and adjustment for treatment, gender and presence of syndesmophytes or ankylosis at baseline (at the patient level). adjOR, adjusted odds ratio; TP, time point; VCI, vertebral corner inflammation; VCFD, vertebral corner fat deposition.

Supplementary table 5. GEE results (adjOR; 95% CI; p values) for the outcome syndesmophyte formation (upper section) and for the outcome syndesmophyte formation or growth of existing syndesmophytes (lower section) according to X-ray reader 1 and reader 2

Definitions of VCI or VCFD	Syndesmophyte formation according to X-ray reader 1 and reader 2	
	Adjustment for within-patient correlation by VU-level and MRI-reader	**Multivariable adjustment***
Definitions based on the presence of VCI and taking the 3 TPs into account		
VCI at baseline, irrespective of inflammation status at other TPs	2.11 (1.27, 3.52); p=0.004	1.90 (1.16, 3.09); p=0.010
VCI at baseline only	2.33 (1.40, 3.90); p=0.001	2.20 (1.34, 3.61); p=0.002
VCI at baseline and another TP	0.68 (0.14, 3.33); p=0.630	0.63 (0.16, 2.49); p=0.507
VCI at any TP	2.09 (1.30, 3.35); p=0.002	1.93 (1.22, 3.05); p=0.005
Definitions based on the presence of VCFD and taking the 3 TPs into account		
VCFD at baseline, irrespective of fat deposition status at other TPs	1.29 (0.79, 2.11); p=0.317	1.18 (0.74, 1.90); p=0.483
VCFD at baseline only	1.22 (0.25, 5.99); p=0.808	1.13 (0.26, 4.91); p=0.868
VCFD at baseline and another TP	1.30 (0.78, 2.17); p=0.311	1.19 (0.73, 1.94); p=0.480
VCFD at any TP	1.74 (1.18, 2.57); p=0.006	1.60 (1.10, 2.33); p=0.014
VCFD at all TPs	1.70 (1.00, 2.88); p=0.050	1.59 (0.96, 2.61); p=0.070
Combined definitions based on the presence of VCI and VCFD and taking the 3 TPs into account		
Sequential or simultaneous presence of VCI and VCFD across the 3 TPs	2.53 (1.49, 4.32); p=0.001	2.29 (1.37, 3.83); p=0.002
Presence of VCI but not VCFD across the 3 TPs	1.25 (0.56, 2.80); p=0.583	1.22 (0.57, 2.60); p=0.609
Presence of VCFD but not VCI across the 3 TPs	1.18 (0.76, 1.85); p=0.463	1.10 (0.72, 1.69); p=0.650
Absence of VCI or VCFD across the 3 TPs	0.57 (0.39, 0.84); p=0.004	0.62 (0.43, 0.89); p=0.009
New VCFD preceded by VCI	3.39 (1.93, 5.95); p<0.001	3.01 (1.76, 5.13); p<0.001
Coexistence of VCFD and VCI at the same TP	0.77 (0.24, 2.46); p=0.653	0.72 (0.25, 2.13); p=0.556

Definitions of VCI or VCFD	Syndesmophyte formation or growth according to X-ray reader 1 and reader 2	
	Adjustment for within-patient correlation by VU-level and MRI-reader	**Multivariable adjustment***
Definitions based on the presence of VCI and taking the 3 TPs into account		
VCI at baseline, irrespective of inflammation status at other TPs	1.83 (1.16, 2.87); p=0.009	1.63 (1.06, 2.50); p=0.027
VCI at baseline only	2.10 (1.34, 3.29); p=0.001	1.95 (1.26, 3.02); p=0.003
VCI at baseline and another TP	0.69 (0.19, 2.55); p=0.575	0.62 (0.20, 1.95); p=0.408
VCI at any TP	1.91 (1.27, 2.89); p=0.002	1.75 (1.17, 2.61); p=0.006
Definitions based on the presence of VCFD and taking the 3 TPs into account		
VCFD at baseline, irrespective of inflammation status at other TPs	1.70 (1.16, 2.49); p=0.006	1.57 (1.09, 2.26); p=0.017
VCFD at baseline only	1.10 (0.27, 4.44); p=0.894	1.04 (0.29, 3.80); p=0.949
VCFD at baseline and another TP	1.67 (1.12, 2.48); p=0.012	1.53 (1.04, 2.23); p=0.030
VCFD at any TP	2.04 (1.47, 2.82); p<0.001	1.85 (1.35, 2.53); p<0.001
VCFD at all TPs	1.91 (1.24, 2.92); p=0.003	1.77 (1.18, 2.66); p=0.006
Combined definitions based on the presence of VCI and VCFD and taking the 3 TPs into account		
Sequential or simultaneous presence of VCI and VCFD across the 3 TPs	2.36 (1.49, 3.74); p<0.001	2.12 (1.36, 3.31); p=0.001
Presence of VCI but not VCFD across the 3 TPs	1.04 (0.50, 2.16); p=0.914	1.00 (0.50, 2.02); p=0.981
Presence of VCFD but not VCI across the 3 TPs	1.49 (1.05, 2.12); p=0.027	1.38 (0.98, 1.93); p=0.064
Absence of VCI or VCFD across the 3 TPs	0.51 (0.37, 0.70); p<0.001	0.56 (0.41, 0.76); p<0.001
New VCFD preceded by VCI	2.40 (1.41, 4.08); p=0.001	2.17 (1.32, 3.56); p=0.002
Coexistence of VCFD and VCI at the same TP	1.20 (0.54, 2.65); p=0.652	1.09 (0.51, 2.30); p=0.829

*Adjustment for within-patient correlation by VU-level and MRI-reader and adjustment for treatment, gender and presence of syndesmophytes or ankylosis at baseline (at the patient level). adjOR, adjusted odds ratio; TP, time point; VCI, vertebral corner inflammation; VCFD, vertebral corner fat deposition.